Granular flow behaviour in the transverse plane of a partially filled rotating cylinder

By A. A. BOATENG† AND P. V. BARR

Department of Metals and Materials Engineering, The University of British Columbia,
Vancouver, BC, Canada, V6T 1Z4

Material flow in partially filled rotating cylinders (rotary kilns) is encountered in many practical applications of material processing, for example incineration, calcination, grain drying, etc. The flow behaviour in the cross-section is important to other transport mechanisms such as mixing and energy distribution within the bed material. The paper describes an experimental study which was carried out with the objective of understanding and improving our predictive capabilities of the rheological behaviour of granular materials in rotary cylinders. Measurement techniques similar to that used in chute flows have been employed to measure flow characteristics, e.g. particle velocities, granular temperature, and solid concentration (in the shear layer developed between the free surface and the bulk of the bed) for different materials having a wide range of coefficients of restitution. The results of the experiments provide the necessary assumptions, constraints, and data for granular flows in partially filled rotating cylinders.

1. Introduction

Bulk granular materials subjected to shearing stress respond by movement of particles within the bulk lattice structure. When the applied stress is low the shear force imparts only minor shifting of the particles but, as the stress increases, significant localized dilation of the structure occurs as individual particles over-ride adjacent particles and deformation of the bulk material occurs along distinct slip planes. When the stress is further increased the diffusion of energy is no longer localized and rapid deformation of the material proceeds *en mass*. The latter is termed granular flow which, because of its importance in both natural phenomena, e.g. avalanches, rockslides, and industrial processing such as gravity flow in chutes and hoppers, has been the subject of considerable study in recent years. The analytical description of granular flow involves aspects of traditional fluid mechanics, plasticity theory, soil mechanics and rheology (Savage 1983, 1984, 1989). It was first recognized by Singh (1978) that energy transport under conditions of rapid deformation in rotary drums occurs primarily by the diffusional effects of particle collisions. Since then it has been demonstrated experimentally that the effectiveness of this diffusional transport is intermediate between that of liquids and gases (Ferron & Singh 1991) and that dilute gas kinetic theory could be employed to describe transport phenomena in granular

† Author to whom correspondence should be addressed; present address: Solite Corporation, PO Box 27211, Richmond, VA 23261, USA.

flows, in this specific case, i.e. mass and heat transfer in the axial direction within a rotary kiln.

The movement of the solids charge in partially filled rotating cylinders, such as rotary kilns, rotary coolers or dryers, can be resolved into two components, i.e. flow in the axial direction imparted by the inclination of the cylinder and that in the transverse plane imparted by rotation. Because particle velocities in the transverse plane, and hence diffusional effects, exceed those in the axial direction by several orders of magnitude, it is the transverse flow which controls the primary bed processes such as heat transfer, particle mixing (and conversely, particle segregation) as well as secondary phenomena such as bed temperature, reaction rates and even rate of advance axially. In fact it was recognized early on (Sullivan, Maier & Ralston 1927; Seaman 1951; Zablotny 1965) that, since axial particle movement occurs only near the upper bed surface, which might be termed the 'active layer', the rate of axial advance will be determined both by the inclination of the cylinder and the rate at which the active layer is renewed, i.e. by the transverse flow. Although granular flow theory has the potential to allow prediction of the granular flow in the transverse plane of a rotary kiln, examples of doing so have only recently appeared, e.g. Savage (1992) for the purpose of replicating existing data on axial segregation of solids beds (Roseman & Donald 1962) and Boateng (1993) who applied thin flow techniques, along with the constitutive relations developed by Lun *et al.* (1984) and Johnson & Jackson (1987), in order to predict velocity profiles and segregation within the active layer. The work reported here embodies an experimental campaign which was mounted for the purpose of obtaining direct measurements of the variables related to granular flows, i.e. the mean particle velocity, the granular temperature and the solids concentration in rotary cylinders. The primary object was to provide guidance in the selection of constitutive relations which might enable granular flow modelling for rotary kilns.

2. Experimental apparatus

The experimental facility employed for granular flow measurements (front end shown in figure 1) comprised a 1000 mm OD (964 mm ID) by 1000 mm rotary drum along with fibre-optic probes employed for measuring local particle velocity. In order to prevent material slippage the smooth steel wall was roughened with a coating of Carboline 801 two-part epoxy paint evenly sprinkled with coarse Ottawa sand having an average particle size of 3.2 mm. The drum was supported on four plastic rollers permanently secured to a steel frame and any tendency of the drum to walk axially was controlled by a thrust bearing at the rear. Electrical power was obtained from a 1/2 HP DC motor with variable speed drive through a chain at the rear of the drum. At the front end of the drum a 16 mm tempered glass panel end-piece was secured to the drum's flange. The end-piece allowed observation of the material within the drum and, through a 250 mm central opening, access for instrumentation. The opening in the end-piece limited the allowable drum loading to 30% which is well in excess of industrial practice. The loading used in the experiments ranged between 3.3% and 29% and in some instances, dependent upon material choice, was limited by the torque of the drive system. The rotational Froude numbers ($\omega^2 R/g$) ranged between 5.4×10^{-4} and 1.3×10^{-2}.

In order to measure particle velocities both within the bed and at the free surface the fibre-optic technique proposed by Savage (1979) and Ahn, Brennen & Sabersky (1991) was employed. This system consisted of two MTI KD 300 Fotonic sensor probes, an
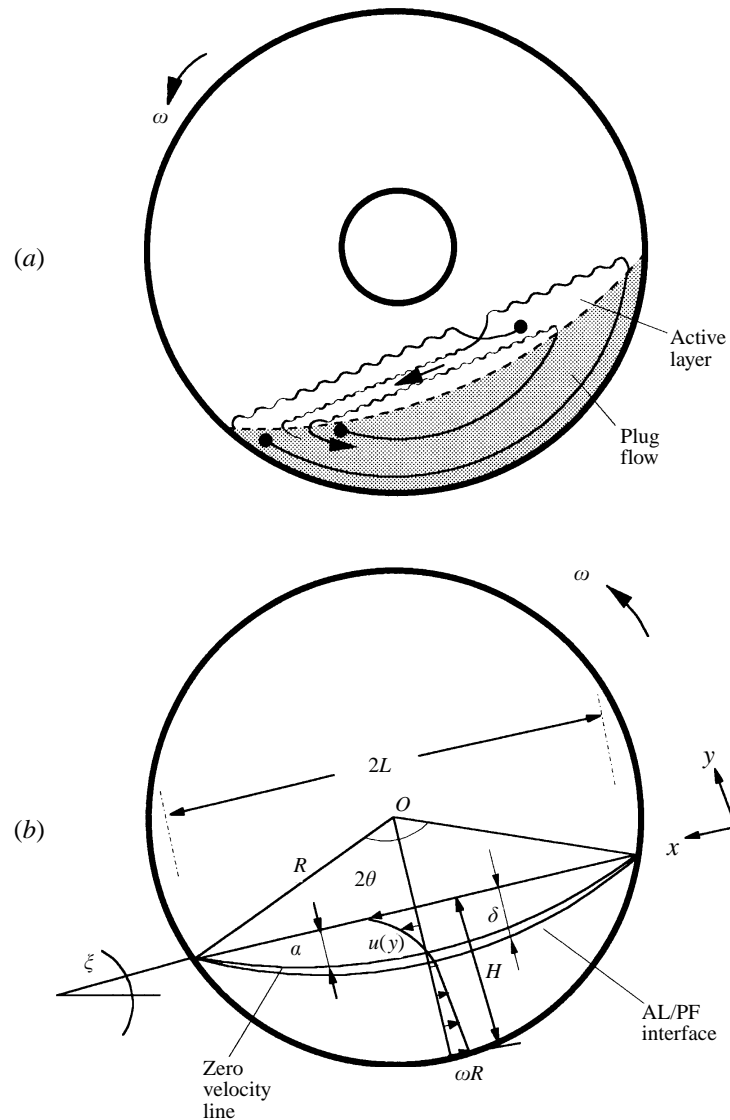
FIGURE 1. Schematic of experimental set-up: (*a*) transverse flow; (*b*) geometry of flow field.

analog HP 3731A cross-correlator along with associated equipment such as a digital ruler for precise placement of the probes, an oscilloscope for visual assessment of the signal, and an X-Y Plotter for graphical output. Each Fotonic sensor-probe unit consisted of a light source connected to the probe tip by a transmitter fibre-optic bundle plus a light sensor which communicates with the probe tip via a second, receiver fibre-optic bundle. In conventional applications a single unit will operate as a displacement transducer by transmitting light to the tip and onto the target. Some portion of this light is reflected back to the tip and, via the receiver bundle, to the sensor with movement of the target being indicated by changes in the character of the reflected light. The passage of a target, such as a particle, past a single Fotonic unit thus produces a characteristic quasi-sinusoidal signal with the peak corresponding to the particle being centred over the tip. In order to measure particle velocities two

probes mounted in parallel and 5 mm apart were employed. When the tip is aligned with the streamwise direction of the flow, the passage of a single particle will produce an (essentially) identical signal in each probe but with a delay in the downstream signal equal to the time required for the particle to travel the separation distance of the probes. In the present work the cross-correlation signals were sent to either an oscilloscope or an X-Y plotter and the time delay between peaks employed for the velocity calculation. Initial calibration of the unit was carried out by sighting the unit onto the disc of a Struers polishing machine rotating at a measured rate and comparing the measured tangential velocity to the theoretical value (ωr) at that radius. In each instance agreement was better than 0.1% which is comparable to the accuracy of the rotation rate measurement. Additional verification of the technique was obtained by sighting on polyethylene particles (one of the bed materials selected for the study) adhered to the end flange of the rotary drum. In this instance agreement was within 0.5–1.0% which is, again, comparable with the accuracy to which the drum rotation rate was controlled.

Velocity measurements were made both at the bed surface (non-intrusively by sighting onto the bed from above) and within the bed burden by traversing downward into the flow normal to the chord length. In both instances misalignment of the probe with the streamwise velocity is a possible source of error, while in the latter instance, distortion of the flow in the vicinity of the probe is also a potential problem. For these reasons the data were routinely checked for adequate closure of the mass balance through the active layer. In addition, traverses into the bed at mid-chord positions were extended well into the plug flow region where the theoretical velocity (ωr) could be used as a check. Both procedures failed to indicate any significant problems due to probe misalignment and/or distortion of the flow field. Two factors appear to mitigate the intrusiveness of the probe: (i) the small size of the tips ($\approx$ 3.25 mm diameter) and (ii) the fact that the target particles were always slightly ahead of the probe tips where flow distortion is least likely to propagate. In order to impart additional confidence to the results, multiple measurements were made for each probe position at each of several sampling times. Subsequent analysis of the data failed to indicate any significant problems. Attempts to measure particle velocities within the bed by sighting through the transparent end-piece were unsuccessful due to interference between the glass and the light signal. Although this problem is correctable by appropriate filtering it was not further pursued, rather measurements made inside the drum enabled assessment of flow distortion in the vicinity of the end-piece by comparing results obtained near the end-piece, from within, to those taken farther into the drum.

3. Physical characterization of the bed material

Although several granular materials were considered for the experimental work, those selected were high-density polyethylene pellets, long grain rice and commercial grade limestone. Among the factors considered in the selection process were (i) a desire to cover a range of particle shapes, i.e. spherical uniformly sized polyethylene pellets, ellipsoidal non-uniformly sized rice grains and unequally shaped and sized limestone particles; (ii) relevance to industrial processes, i.e. grain drying and limestone calcination, and (iii) ease of characterization, i.e. polyethylene pellets. Although the polyethylene pellets are quite atypical of rotary kiln or dryer feedstock this material is well suited to any mathematical modelling that might ensue from the experimental work. Furthermore, the material has been extensively employed in granular flow

Material	Av. d_p	ρ_p	ϕ	e_p	e_w
	(mm)	(kg m^{-3})	(deg.)	-	-
Polyethylene	3.63 ($\pm$0.02)	960	25	0.85	0.70
Limestone	3.22 ($\pm$1.23)	3730	35	0.60	0.50
Rice grain	5.35 ($\pm$0.01)	1046	32	-	-

TABLE 1. Estimated relevant properties of material used.

studies (e.g. Ahn *et al.* 1991; Johnson & Jackson 1987; Savage 1979, etc.) and any results generated with it can serve as a check on the results produced by other materials.

Physical characterization of the three materials involved the measurement of the particle size, particle density, static angle of repose, ϕ, of the particle ensemble within the test drum and the coefficient of restitution (both interparticle, e_p, and particle-to-wall, e_w). These data are summarized in table 1. The angle of repose was determined in the manner suggested by Henein, Brimacombe & Watkinson (1983*a*) and is the maximum angle subtended by the bed surface (from the horizontal) during slow rotation of the drum. This maximum angle is a measure of the lattice structure's ability to transmit shear loads, which is, in turn, determined by the ease with which particles can over-ride others within the lattice. Thus the spherical polyethylene pellets exhibit a relatively low angle of repose (25°) compared to the ellipsoidal rice grains (32°) or the irregular limestone particles (35°). In the particular case of flow in the transverse plane of the rotary drum, the potential energy imparted to individual particles by the rotation of the drum (and which therefore must be dissipated by the granular flow established within the active layer) is proportional to the angle of repose. Dissipation of energy within the active layer may be dominated (Lun *et al.* 1984) by interparticle collisions and thus the coefficient of restitution (especially particle-to-particle, e_p) is an important rheological parameter. Unfortunately e_p is difficult to measure with accuracy and the values appearing in table 1 were obtained using the approximate method of Sondergaard, Chaney & Brennen (1990) which involves measurement of the rebound height for particles dropped onto a plane surface formed from the same material. In the case of the polyethylene pellets the e_p value of 0.85 given in table 1 is identical to that reported by Johnson & Jackson (1987). Values of e_w shown in table 1 were obtained by rebounding particles off the drum wall and, owing to the resilience of the epoxy coating, are somewhat lower than the corresponding particle-to-particle values.

4. Experimental parameters and data analysis

The variables employed for the experimental program were the material rheology, i.e. polyethylene pellets, rice grains and limestone particles; the drum loading (expressed as the percentage of the drum cross-sectional area occupied by the bed material and subsequently referred to as percent fill); and the drum rotation rate. Although these do not exhaust all possibilities, for example drum size, particle size or the ratio of drum diameter to particle diameter might also be examined, the set of variables used was considered sufficient to meet the objectives of assessing the constitutive relations proposed for granular flows. The test work targeted several rotation rates, 1–5 r.p.m., while drum loading was varied from a low of 3.3% to a high of 29%, the majority being in the 8% to 15% range which is typical of industrial

Fill (%)	3.3	8.5	10	15	29
H (cm)	7 (±0.2)	13.5 (±0.3)	15 (±0.5)	20 (±0.5)	31 (±0.5)
$2L$ (cm)	50 (±1.0)	65 (±1.5)	70 (±1.0)	77 (±1.8)	90 (±0.5)

TABLE 2. Geometry of bed for run conditions.

kiln operations. However, not all combinations of material, rotation rate, and percent fill were possible due to power limitations on the drive motor. Polyethylene was run on a wide range of drum loadings (3.3%, 8.5%, 15%, and 29%) and operated at the full range of rotational rates. Rice grains were loaded at 3.3%, 8.5%, and 10% fills and operated at 3 and 5 r.p.m. only. Table 2 shows the geometrical bounds of the loading conditions. Deeper bed loadings were not possible for rice grains since these resulted in a slipping bed motion. The same limitations applied to limestone which was operated at a slightly wider speed range (between 2 and 5 r.p.m.) but at bed loadings not exceeding 8.5%. When assessed on the basis of the bed behaviour diagrams developed by Henein *et al.* (1983*a, b*) the test conditions should have generated either a rolling mode of bed motion, which was in fact the case, or, in a few instances of higher rotation rates, a cascading bed, which was never observed.

The parameters to be derived from the data were those which are pertinent to the application of granular flow constitutive relations to flow in the transverse plane of a rotary drum, i.e. the mean particle velocity parallel to the bed surface, the granular temperature and the solid fraction. These parameters are required only for the active (shear) layer near the bed's free surface. However, since the extent of the active layer is not known *a priori*, an additional parameter to be measured is the active layer depth as a function of position along the chord length subtended by the bed surface (see figure 1). Thus a complete mapping of the flow within the active layer also involved numerous probe positions within the plug flow region in order to ascertain the location of the active layer/plug flow interface. Typically about 25 individual probe positions were required in order to characterize the active layer.

The raw data gathered at each probe position comprised the cross-correlated signals generated by the passage of individual particles past the probe unit. The mean particle velocity was obtained by time averaging a sufficient number of individual signals so that a stable value was achieved. The velocity fluctuation u'^2 was calculated from the variance and, as suggested by Ahn *et al.* (1991), was related to one component of the granular temperature as

$$\tilde{T} = (u'^2)^{1/2}. \tag{1}$$

The third parameter obtained from the data, the solids fraction, is a measure of the dilation which accompanies the transition from the rigid lattice of the plug flow region to the granular flow regime in the active layer. An approximation of the solids linear concentration, ϑ, was obtained from the probe data through the formula (Ahn *et al.* 1991)

$$\vartheta = d_p C_{sp}. \tag{2}$$

In (2), d_p is the mean particle diameter and C_{sp} is the characteristic particle spacing (Ahn *et al.* 1991) obtained by dividing the number of particles passing the probe location (per unit time) by the mean particle velocity at that location.

The determination of the active layer depth was complicated by the reversal of particle flow which occurs in the vicinity of the interface between the active and the

plug flow regions. Because the probe is unable to accurately measure very low or null particle velocities (i.e. low particle counts) the position of the interface was obtained by extrapolating particle count profiles (normal to the bed surface) constructed in both regions to their respective zero intercept. As can be seen in figures 4 and 5 shown later, both intercepts are essentially coincident. Additional manipulation of the data included determination of the bulk (average) streamwise velocity in the active layer, u_δ, and the mass flow in both the active layer and plug flow region. The bulk velocity was obtained according to

$$u_{\delta,x} = \frac{\sum_{i=1}^{N_\delta} u_{x,i}(\Delta Y)}{\sum_{i=1}^{N_\delta} (\Delta Y)_i} \tag{3}$$

where N_δ is the number of probe positions (normal to the bed surface) within the active layer at each position, x, along the chord length and ΔY is the distance between probe positions. Values of N_δ ranged from about 20 at mid-chord position to about 5 near the apex. The mass balances were also carried out at various positions along the chord length in order to provide a global check (or closure) for both the velocity and active layer depth results. The expressions employed were, for the active layer and plug flow regions respectively,

$$\dot{m}_{al} = \rho_p \vartheta_{x,al} \sum_{i=1}^{N_\delta} u_{x,i} \Delta Y, \tag{4}$$

$$\dot{m}_{pf} = \rho_p \vartheta_{pf} \omega \int_{R_{IF}}^{R_w} r\,\mathrm{d}r, \tag{5}$$

$$\dot{m}_{pf} = \rho_p \vartheta_{pf} \omega (R_{IF}^2 - R_w^2), \tag{6}$$

where R_{IF} is the radial distance from the drum's centreline to the active layer/plug flow interface and R_w is the drum radius.

5. Results and discussion

It was the primary objective of the work to determine, for the specific case of flow in the transverse plane of a rotary drum, the parameters associated with granular flow theory, i.e. mean particle velocity, granular temperature and solid concentration. It is useful, however, to open with a more general discussion of the results beginning with the effects of the end-piece. Although previous studies have frequently relied upon sightings taken through a transparent cap the localized distortion of the flow caused by an additional surface has never been established. In the present work the dynamic angle of repose, ξ, was observed to increase gradually, beginning at about 10 cm ($\approx$ 30 particle diameters in the case of the polyethylene pellets) from the end-piece and axially toward the glass. The end-piece effect increased the angle subtended by the material by about 10% over that of the undisturbed region. In order to quantify this effect on the flow field surface velocity measurements were made at an axial distance of 5 cm from the end-piece which were then compared with values obtained for the undisturbed region at 22 cm from the end-piece. Representative results given in figure 2(a) for polyethylene pellets (at 15% fill and 5 r.p.m.), show that the increased angle
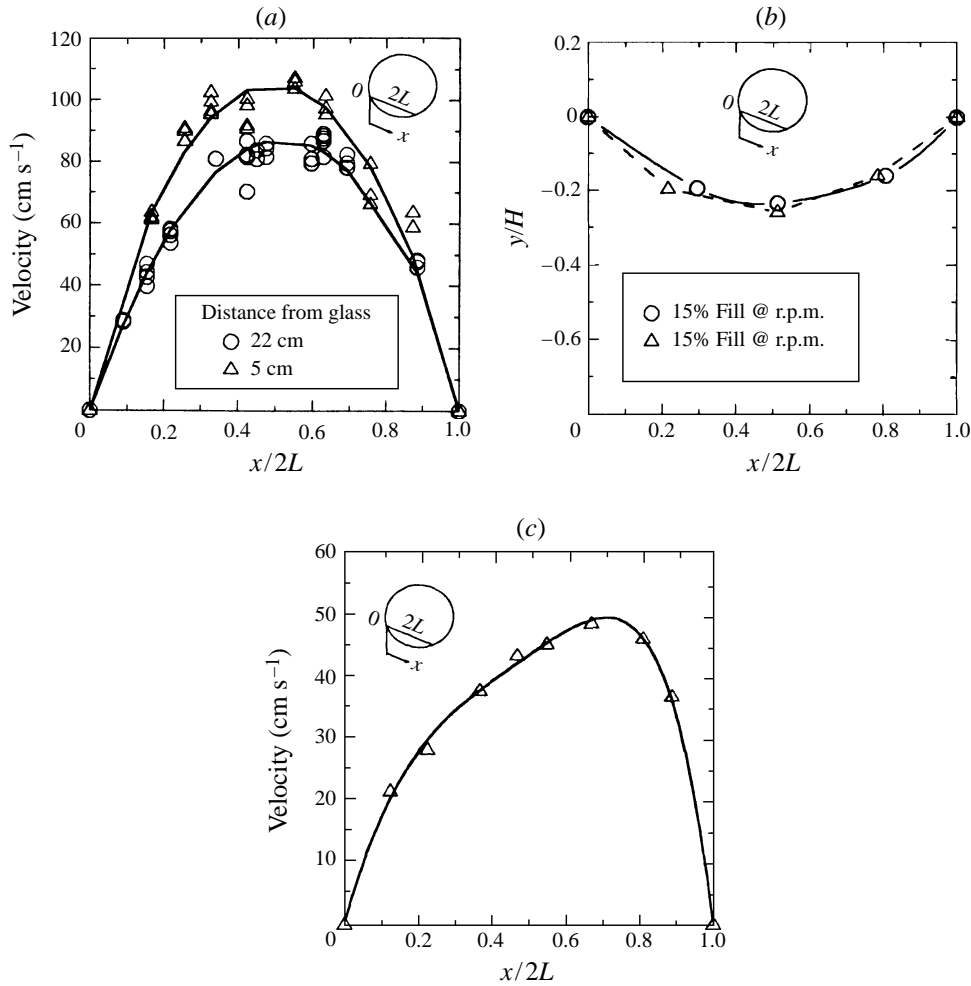
FIGURE 2. Surface velocity and depth profile shapes for polyethylene. (*a*) End-piece effect (15% fill, 5 r.p.m.); (*b*) active layer depth; (*c*) skewed velocity profile (3.3% fill, 5 r.p.m.).

of repose near the end-piece provides an added enhancement of particle movement as is depicted by significantly higher velocities in the active layer. Owing to gravitational effects velocities increased by about 20–25% in this instance. It might be noted that this is counter to measurements obtained for chute flows (Ahn *et al.* 1991) which suggest retardation of the flow within the active layer by the end-piece.

The extent of the active layer was determined both in the vicinity of the end-piece and in the undisturbed region for a variety of conditions. Figure 2(*b*) which is shown for polyethylene pellets (15% fill, 3 r.p.m., and 8.5% fill, 2 r.p.m.) is representative of the larger body of results which defines the active layer shape. These measurements suggest that the depth of the layer, as determined visually through an end-cap, i.e. Henein *et al.* (1983), Pershin (1988) or Gauthier (1991), could be about 15% less than that in the undisturbed flow region. It is of interest to note that, although other aspects of the flow, for example the shape of the surface velocity profile and the velocity profile traversing normal to the bed surface, showed significant variation, the active layer retained the (approximately) symmetric parabolic shape under all test conditions for

this material. As suggested by Gauthier (1991), the active layer thickness, if evaluated as a percentage of the bed depth at mid-chord ($\delta/H \times 100\%$), can be expected to increase with rotation rate (drum loading held constant) and decrease with drum loading (rotation rate maintained constant). Previous experimental work by Singh (1978) using polyethylene pellets in rotary drums had suggested that the velocity at the free surface of the active layer would be parabolic centred on the mid-chord position. However the symmetric surface velocity distribution exhibited (e.g. figure 2*a*) was not consistent for all materials tested or even for the same material at different rotation rates or fill levels. For example reducing percent fill from 15 to 3.3 while holding material type (polyethylene pellets) and rotation rate constant (5 r.p.m.) shows the velocity profile skewing towards the base (figure 2*c*) i.e. particles continue to accelerate well past the mid-chord position. In the case of rice grains (shown later in figure 6) the situation can be more complex; particles which align themselves parallel to the wall, when discharged onto the bed surface near the apex do realign parallel to the bed surface. Associated with this is a rapid initial acceleration of the grains, followed by an equally rapid deceleration, all occurring within the initial 30% of the chord length. Such unstable conditions are related to the rheological properties of the material and will be discussed later.

When considered in terms of granular flow theory it is not only the local values of the particle velocity, granular temperature and solids concentration which are of interest. Also of interest is the local variation of each parameter, in particular the gradient normal to the bed surface. Typical results of the latter are presented in figure 3. Evident in these results is the similarity in profile shapes irrespective of position along the chord length. Such behaviour can expedite mathematical modelling of the flow field since it lends itself to valuable simplifications found in the analysis of thin flows, e.g. boundary layer type flows. Owing to this and also in order to avoid excessive detail the discussion will focus on conditions at mid-chord position and conditions at other points along the chord length will be considered only when they show a significant variation. Similarly polyethylene pellets will be used as the reference material and the behaviour of rice grains and limestone will be described chiefly in terms of any dissimilarities to that of the pellets.

Surface and depth profiles of the streamwise particle flow characteristics are summarized in figures 4–6. In order to facilitate comparisons some of the results are normalized using the total bed depth (H), chord length ($2L$) and the tangential velocity at the inside wall surface (ωR_w). We begin the discussion with the depth profiles by considering typical results shown in figure 4. Although Savage (1979) had obtained parabolic velocity profiles for the flow of polyethylene pellets down a roughened chute, those in the active layer were essentially linear except very near the bed surface and in the region of the interface with the plug flow region. Thus, through much of the active layer, the shear rate is essentially uniform (i.e. du/dy is constant).

Taken in total the results obtained for polyethylene pellets suggest that the primary feature of the granular flow in the active layer is that of uniform shear normal to the free surface. This was not, however, confirmed by the results obtained for the other materials. At low drum loading all three materials exhibited essentially linear velocity profiles at the mid-chord position. At higher drum loadings, however, the non-spherical materials developed fuller, more parabolic velocity profiles as shown in figure 5(*c*), the departure from linearity tending to increase with rotation rate (for constant drum loading). The development of these parabolic velocity profiles suggests that the shear stress only tends to zero at the free surface ($du/dy = 0$) as the thickness of the active layer increases with rotation rate. Under these conditions particles within
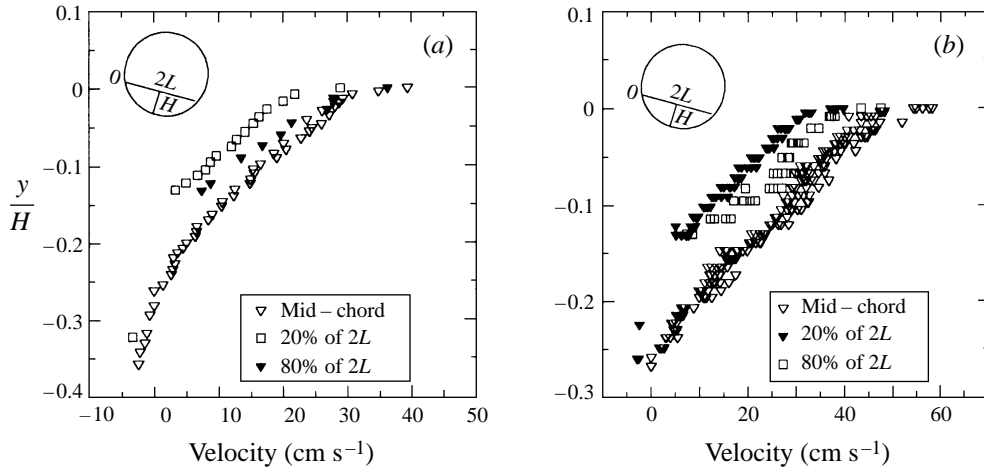
FIGURE 3. Average particle velocity as a function of bed depth at different surface locations showing similarities in profile irrespective of surface position: (*a*) polyethylene, 8.5% fill, 2 r.p.m.; (*b*) polyethylene, 15% fill, 3 r.p.m..
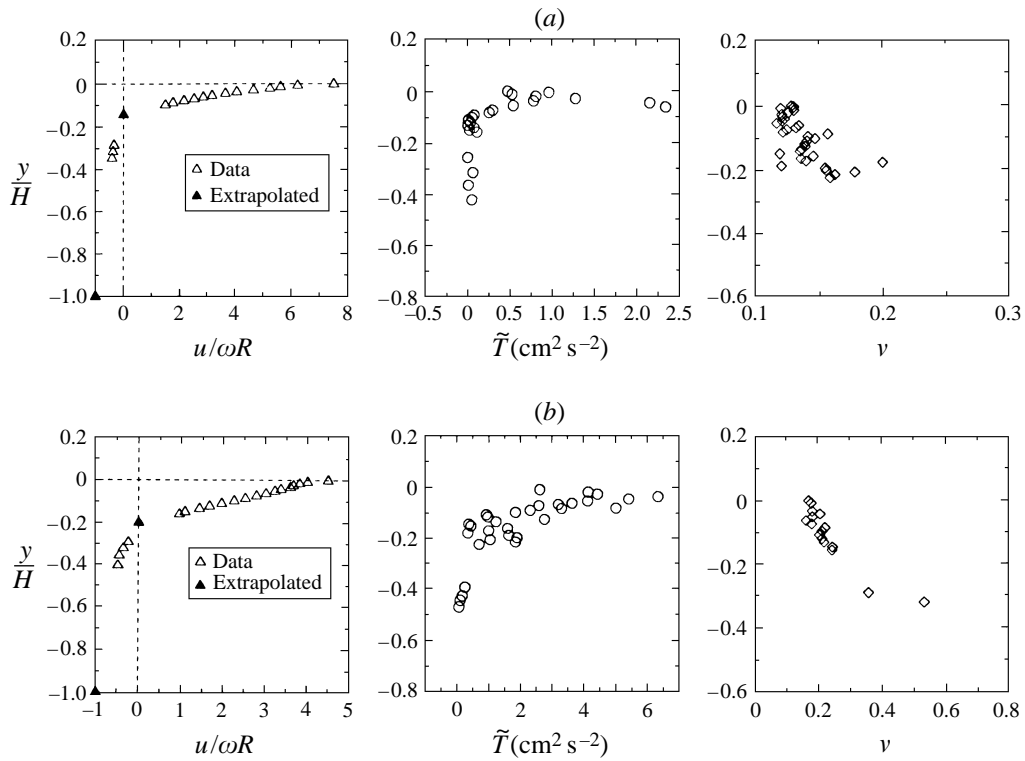

FIGURE 4. Velocity, granular temperature and solids concentration as function of depth (radial traverse at mid-chord) for polyethylene pellets at 29% fill: (*a*) 1 r.p.m.; (*b*) 5 r.p.m..
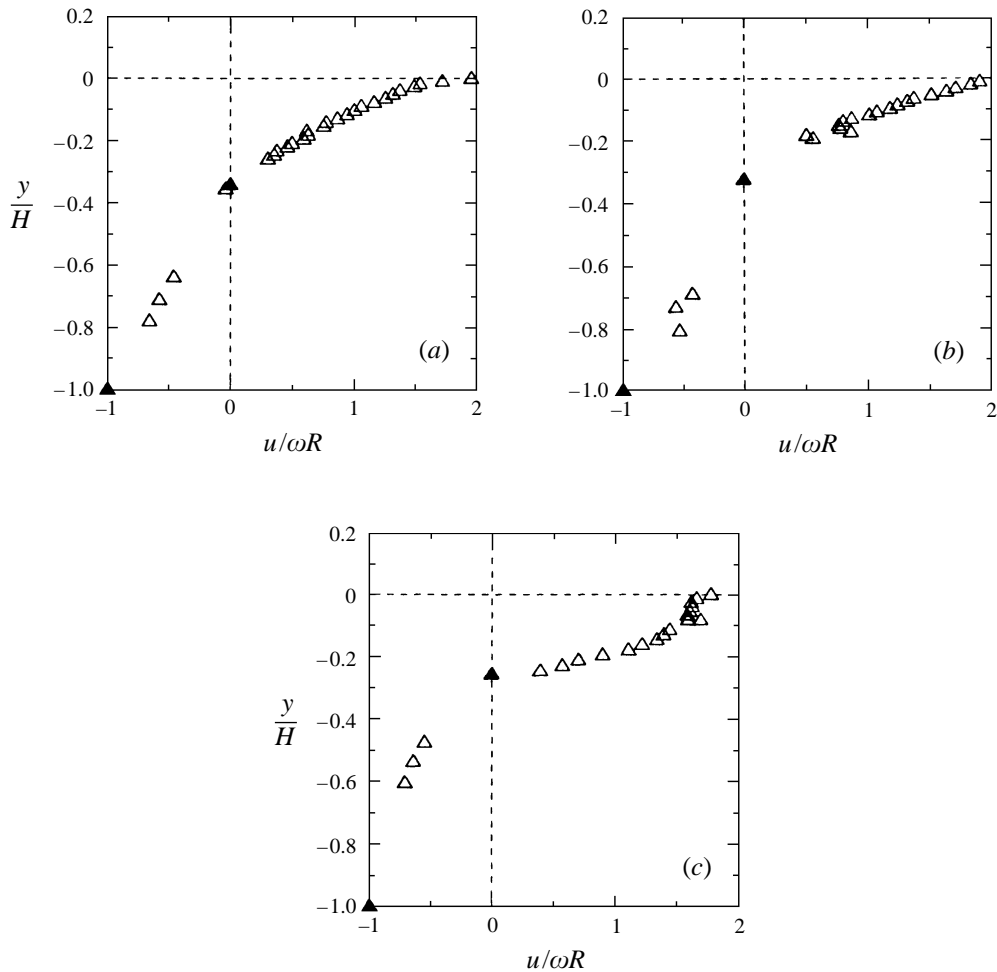
FIGURE 5. Effect of rheology and rotational rate on velocity profile: (*a*) polyethylene (3.3% fill, 3 r.p.m.); (*b*) long-grain rice (10% fill, 3 r.p.m.); (*c*) long-grain rice (10% fill, 5 r.p.m.).

the shear layer tend to move *en bloc* without deformation. As suggested earlier, the granular temperature (equation 1) is a measure of the fluctuation in the local particle velocity and is analogous (Zhang & Campbell 1992) to the thermodynamic temperature as derived from dense-gas kinetic theory. Although the data in figure 4(*b*) exhibit considerable scatter it is evident that the granular temperature increases rapidly near the free surface which is consistent with both the physical situation and Couette flow modelling results of Zhang & Campbell (1992). The low values observed for $\tilde{T}$ are partly due to low particle shear rates for the rotation speeds studied and the fact that only one of the three components of the variable could be measured. The linear solids concentration can be expected to decrease in the active layer due to the dilation which accompanies the transition from rigid-body motion in the plug flow region to granular flow in the active layer. Although, again, considerable scatter is evident in the data (figure 4*c*) the solids concentration increases from a minimum at the free surface to the level of incipient dilation at the interface between the active layer and the plug flow region.

The observed behaviour of the flow field might be explained by physical interpretation of the data for granular temperature and linear concentration in the active layer, i.e. there is a bulk viscosity which is proportional to the solids concentration, ϑ, and shear viscosity, μ. The latter is, in turn, proportional to granular temperature and granular conduction. Hence, as has been suggested by the work of Davies (1986) for similar flows, the flow within the active layer should mimic, depending upon the material rheology and shear rate, pseudoplastic (indicated by perhaps slightly convex velocity profiles exhibited by the polyethylene pellets) to Newtonian (linear velocity profiles) and to dilatant (concave velocity profiles) as the strain rate increases. This suggests the possibility that shearing and unshearing flow regimes coexist in the same flow field. Therefore the stress tensor associated with flow might comprise a combination of static and kinetic components with the relative importance of each contribution relating to the extent to which the is drum rotated.

Because of the relatively high frictional forces which can be generated between individual particles of materials other than polyethylene, surface velocity profiles exhibited in figure 6 conform to an order–disorder behaviour as particles discharge from the plug flow region into the active layer. This is because a large amount of energy is required to overcome static stresses as is evidenced by the build-up of material at the apex. In this region the granular temperature is low due to the inelasticity of the particle collisions. The first appearance of the 'fluidized' behaviour as the material yields near the apex can be expected to follow the Mohr–Coulomb (Zhang & Campbell 1992) failure criterion (i.e. $\tau_{xy} = \tau_{yy} \tan \xi$) where the normal stress is simply the overburden, as defined by the concentration of particles. Since the energy is not self-sustaining in granular materials it is transferred downward as kinetic energy of the mean flow. Bearing in mind that in a field of granular transport, the granular temperature, however small, plays the same role as thermodynamic temperature plays in kinetic theory of dense gases, it should be expected that the granular temperature is greatest in the regions where the material exhibits fluid-like behaviour and lowest in those regions where the behaviour is solid-like (Zhang & Campbell 1992). Thus the results shown in figure 6(a) would indicate what might be described as granular conduction in the flow direction (i.e. from the apex to the base). From works relating Couette granular flow, at least it can be said the mechanism by which 'granular' energy is generated may be attributed to shear work on the control volume (see Zhang & Campbell 1992) and can be defined as the product of the shear stress and the shear rate ($\tau_{xy} \mathrm{d}u/\mathrm{d}y$). At the locations where the velocity goes to zero, the shear work goes to zero, but the stress ratio ($\tau_{xy} = \tau_{yy} \tan \xi$) is not zero, and therefore, $\mathrm{d}u/\mathrm{d}y \to 0$, resulting in low granular temperature. As a result, the fluid-like behaviour changes to solid-like behaviour whereby a few particles at the free surface form a non-shearable structure. One evidence of inadequate energy dissipation (inelastic dissipation) is the possibility of multiple velocity peaks, figure 6(b), giving rise to wave-like formations on the exposed bed surface. Here two or more velocity peaks may form on the bed surface in contrast to the single peaks shown for polyethylene pellets (symmetric or skewed distribution).

The formation of multiple parabolic profiles can be attributed to instabilities which develop as a result of granular energy dissipation; this behaviour has a strong dependence on the solid fraction (concentration) and the coefficient of restitution of the material (see, e.g., Savage 1992). Hence, except for very deep beds, polyethylene pellets can be expected to develop 'singular' surface velocity profiles either symmetrical about the mid-chord plane or skewed. In terms of material rheology such behaviour may account for the fact that polyethylene pellets, as a result of their high coefficient
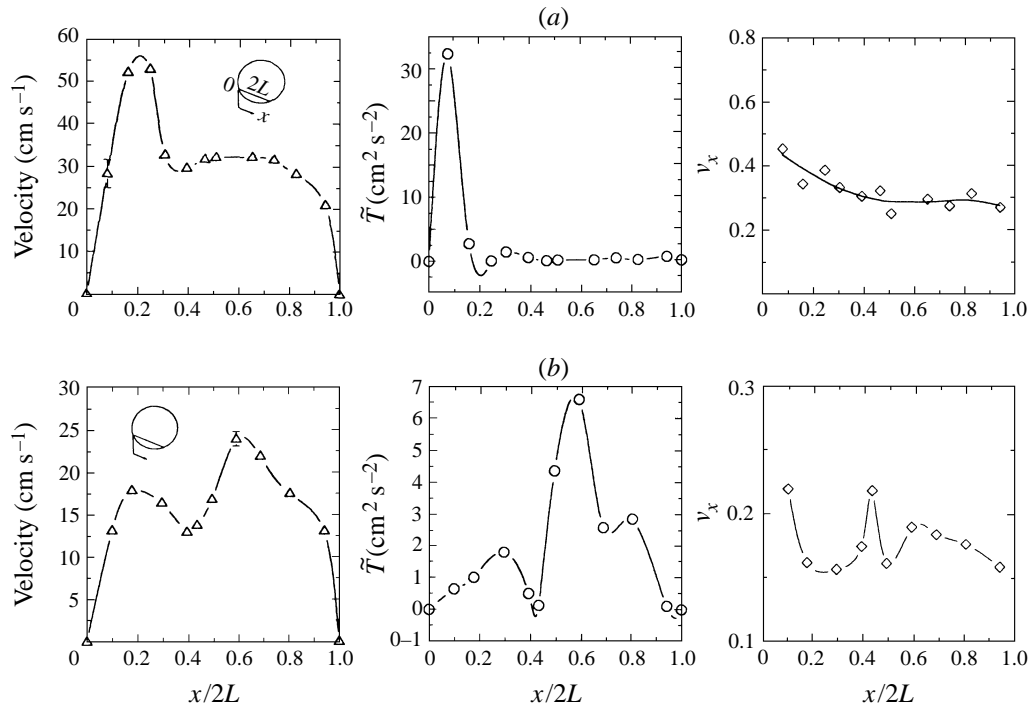
FIGURE 6. Surface velocity, granular temperature and solids concentration: (*a*) long-grain rice (10% fill, 5 r.p.m.); (*b*) limestone (3.3% fill, 2 r.p.m.).

of restitution, more readily dissipate their energy than rice grains or limestone. The collisional inelasticity, which gives rise to the build-up of material at the apex for rice grains and limestone, is relatively weaker in polyethylene (i.e. stronger elastic collisions). A symmetric surface velocity profile observed for polyethylene pellets indicates that particle flux into the active layer equals that leaving it. Such a criterion may, therefore, be invoked to close the mathematical modelling of the flow field.

The data relating active layer depth to material type, rotation rate and degree of fill are presented in figures 7 and 8. It is useful to attempt an explanation of these in terms of the rheological behaviour of granular flows. In failure zones, such as the active layer of the bed, the Mohr–Coulomb yield criterion, i.e. the ratio of the shear to normal stress is constant ($\tau_{xy} = \tau_{yy} \tan \xi$), applies irrespective of the degree of agitation. In the intermediate regime of shearing and unshearing flow the collisional contribution of the shear stress can still be related to the velocity gradient in a manner analogous to Reynolds stresses in fluids, i.e. $\tau_{xy} \approx (\mathrm{d}_p \mathrm{d}u/\mathrm{d}y)^2$. Therefore, that component of the shear stress will be proportional to the rotation rate and, in order to maintain the constancy established by $\tan \xi$, the normal stress must increase. However, the normal stress is simply the overburden pressure which is, in turn, proportional to the thickness of the active layer. Therefore increasing the rotation rate can be expected to increase the volume of material or the number of particles in the shear layer. This analysis is not new; it has been made for other granular flow applications (see, e.g., Johnson & Jackson 1987). When expressed as a function of percentage of the total drum cross-section, the drum loading varies with chord length and drum radius (see,
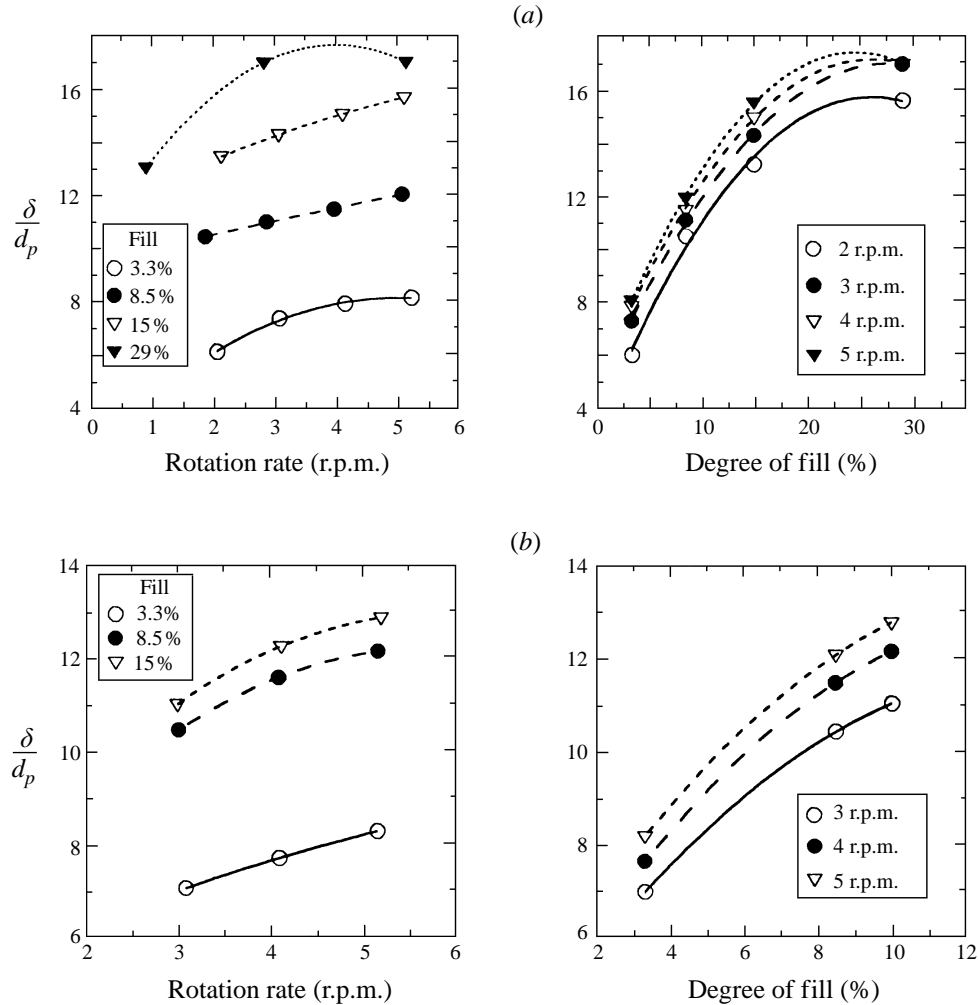
FIGURE 7. Active layer depth as a function of rotation rate and drum loading:
(*a*) polyethylene; (*b*) long-grain rice.

e.g., Ferron & Singh 1991) according to

$$f = \frac{1}{\pi} \left[\sin^{-1} \left(\frac{2L}{R} \right) - 2L \left(1 - \left(\frac{2L}{R} \right)^2 \right)^{1/2} \right]. \tag{7}$$

This relationship explains why beyond a specified degree of fill the chord length is relatively insensitive to drum loading although the number of particles sheared increases. In the Couette shear flow experiments of Johnson & Jackson (1987) it was demonstrated that, beyond some critical value, increasing the outer wall speed of an annulus would not force any more material to enter into the shear layer. In that work the shear layer depth was reported to be about 23% which compares well with the results presented here.
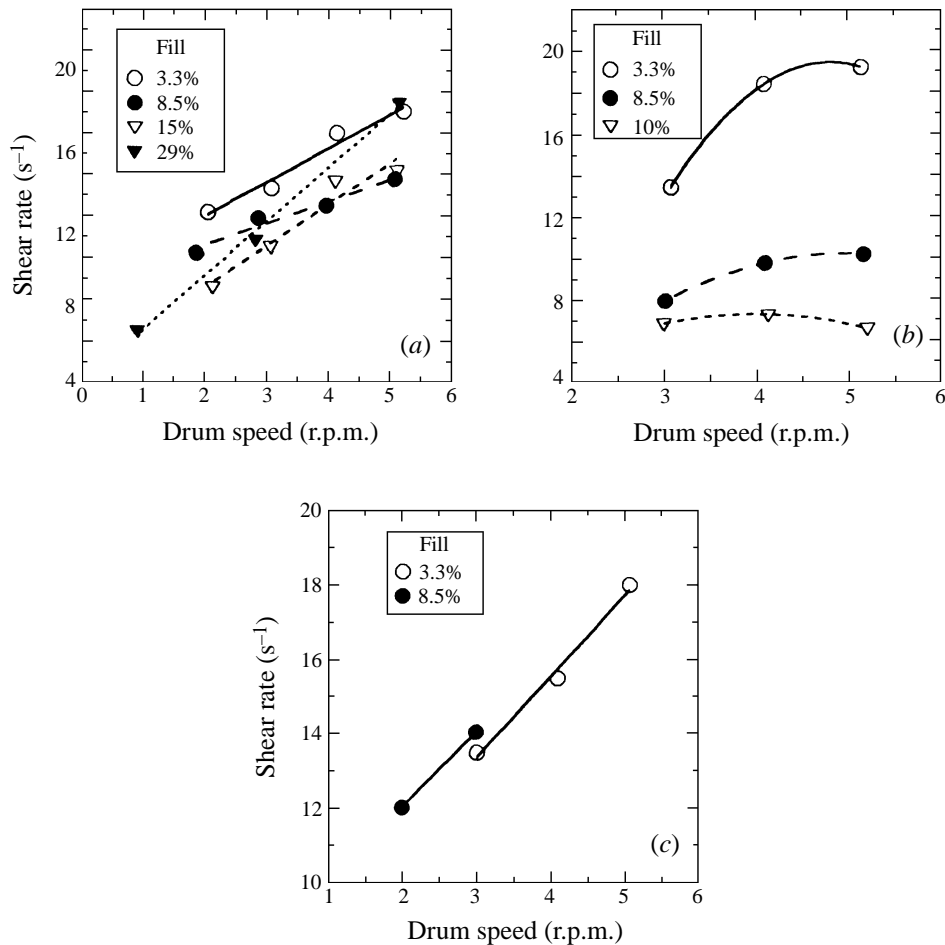
FIGURE 8. Mean shear rate, du/dy, in the active layer as a function of rotation rate and drum loading: (*a*) polyethylene pellets; (*b*) long-grain rice; (*c*) limestone.

6. Summary and conclusions

Experiments on the continuous flow of granular material in the transverse plane of a rotating drum have been carried out with the aim of understanding the rheological behaviour of materials in rotary kilns. The granular materials employed, which varied substantially in physical properties, were polyethylene pellets, long-grain rice, and limestone. The rotary drum comprised a steel cylinder of 964 mm ID (1000 mm OD) and 1000 mm long having a glass end-piece with a centre opening providing an access port for flow measurements. Optical-fibre probes were used to measure mean particle velocities both within the bed and at the bed surface. From these data the granular temperature and the linear concentration of particles were computed.

For the drum speeds and the degrees of fill studied, the flow field could be characterized as that of the intermediate Bagnold regime where shearing and unshearing flow may coexist in the same flow field. As in all granular flows there is a bulk viscosity of the flow which is directly proportional to the shear viscosity and dilation and is also inversely proportional to particle size. The shear viscosity is proportional to the granular temperature, a field property which is a measure of kinetic energy

and is, in turn, a function of the coefficient of restitution of the granules. There is also granular conduction in the shear or active layer. As a result the shear layer grows with increased shear rate or rotational rate and decreases with increased bed depth. Because the radial distribution function for the flow field is dependent upon concentration there is a maximum shearable concentration beyond which there is no further shearing. Thus, depending on the coefficient of restitution and the rotational rate, the velocity profiles in the radial direction may mimic pseudoplastic, Newtonian, or dilatant plastic. Such behaviour suggests that the stress tensor might comprise a combination of static and kinetic (streaming and collisional) and that the rotary kiln cross-sectional flow field may be modelled by constitutive relations of Lun *et al.* (1984). However, one must combine these stress components as suggested by Johnson & Jackson (1987).

REFERENCES

AHN, H., BRENNEN, C. E. & SABERSKY, R. H. 1991 Measurements of velocity, velocity fluctuation, density, and stresses in chute flows of granular materials. *Trans. ASME J. Appl. Mech.* **58**, 792–803.

BOATENG, A. A. 1993 Rotary kiln transport phenomena: study of the bed motion and heat transfer. PhD dissertation, University of British Columbia, Vancouver.

DAVIES, T. R. H. 1986 Large debris flow: A macro-viscous phenomenon. *Acta Mechanica* **63**, 161–178.

FERRON, J. R. & SINGH, D. K. 1991 Rotary kiln transport processes. *AIChE J.* **37**, 758–774.

GAUTHIER, C. 1991 Etude du movement granulaire dans cylindre en rotation. MSc thesis, Universite du Quebec a Chicoutimi, Canada.

HENEIN, H., BRIMACOMBE, J. K. & WATKINSON, A. P. 1983*a* Experimental study of transverse bed motion in rotary kilns. *Metall. Trans.* B **14**(6), 191–205.

HENEIN, H., BRIMACOMBE, J. K. & WATKINSON, A. P. 1983*b* The modelling of transverse solids motion in rotary kilns. *Metall. Trans.* B **14**(6), 207–220.

JOHNSON, P. C. & JACKSON, R. 1987 Frictional-collisional constitutive relations for granular materials, with application to plane shearing. *J. Fluid Mech.* **176**, 67–93.

LUN, C. K. K., SAVAGE, S. B., JEFFREY, D. J. & CHEPURNIY, N. 1984 Kinetic theories for granular flow: inelastic particles in Couette flow and slightly inelastic particles in a general flow field. *J. Fluid Mech.* **140**, 223–256.

PERSHIN, V. F. 1988 Energy method for describing granular motion in a smooth rotating cylinder. *Teoreticheskie Osnovy Khimicheskoi Tekhnologii* **22**(2), 255–260.

ROSEMAN, B. & DONALD, M. B. 1962 Effects of varying the operating conditions of a horizontal drum mixer. *Brit. Chem. Engng* **7**(11), 823–827.

SAVAGE, S. B. 1979 Gravity flow of cohesionless granular materials in chutes and channels. *J. Fluid Mech.* **92**, 53–96.

SAVAGE, S. B. 1983 Granular flow down rough inclines - review and extension. In *Mechanics of Granular Materials: New Models and Constitutive Relations* (ed. J. T. Jenkins & M. Satake), pp. 261–282. Elsevier.

SAVAGE, S. B. 1984 The mechanics of rapid granular flows. *Adv. Appl. Mech.* **24**, 289–366.

SAVAGE, S. B. 1989 Granular flow materials. In *Theoretical and Applied Mechanics* (ed. P. Germain, M. Piau & D. Caillerie), pp. 241–266. Elsevier.

SAVAGE, S. B. 1992 Instability of unbounded uniform granular shear flow. *J. Fluid Mech.* **241**, 109–123.

SAVAGE, S. B. & JEFFREY, D. J. 1981 The stress tensor in a granular flow at high shear rates. *J. Fluid Mech.* **110**, 225–272.

SEAMAN, W. C. 1951 Passage of solids through rotary kilns: factors affecting time of passage. *Chem. Engng Prog.* **47**(10), 508–514.

SINGH, D. K. 1978 A fundamental study of the mixing of solid articles. PhD dissertation, University of Rochester, Rochester.

SONDERGAARD, R., CHANEY, K. & BRENNEN, C. E. 1990 Measurements of solid spheres bouncing off flat plates. *Trans. ASME J. Appl. Mech.* **57**, 694–699.

SULLIVAN, I. D., MAIER, C. G. & RALSTON, D. C. 1927 Passage of solids particles through rotary cylinder kilns. *US Bureau of Mines Tech. Rep.* 384.

ZABLOTNY, W. W. 1965 The movement of the charge in rotary kilns. *Intl Chem. Engng* **5**(2), 360–366.

ZHANG, Y. & CAMPBELL, C. S. 1992 The interface between fluid-like and solid-like behaviour in two-dimensional granular flows. *J. Fluid Mech.* **237**, 541–568.